Investigation on the Effect of Activating Flux on Tungsten Inert Gas Welding of Austenitic Stainless Steel Using AC Polarity

Suman Saha[1] and Santanu Das[2]
Department of Mechanical Engineering, Kalyani Govt. Engineering College,
Kalyani - 741235, West Bengal, India
E-mail: [1]sumansaha.me@gmail.com, [2]sdas.me@gmail.com

DOI : 10.22486/iwj/2018/v51/i2/170313

ABSTRACT

Tungsten Inert Gas (TIG) welding is a popular joining process due to its inherent capability in producing superior quality welding in a wide range of materials. However, lower productivity of it paves the way for introduction of a number of variants of TIG welding, including Flux Bounded TIG (FB-TIG) welding and Activated TIG (A-TIG) welding. In this paper, variations of weld morphology and characteristics with heat input in AC A-TIG welding of both bead-on-plate and butt joining of 6mm thick 316L stainless steel plates using TiO_2, Cr_2O_3 and Fe_2O_3 as activating flux and a stainless steel filler material are investigated. Results are also compared with that obtained in conventional TIG welding. Variations of various weld characteristics viz. depth of penetration, width of weld bead, reinforcement, Reinforcement Form Factor (RFF), and Penetration Shape Factor (PSF) against change in heat input are analyzed and compared. It is observed that TiO_2 and Fe_2O_3 fluxes effectively enhance the penetration due to increase in fluidity and wettability of molten metal and, at the same time, reduce the width of weld bead; whereas, Cr_2O_3 flux gives inferior results as it reduces penetration instead of increasing it as compared to conventional TIG welding.

Keywords : Welding; A-TIG; Activated Flux; Heat Input; Depth of Penetration.

1.0 INTRODUCTION

Low productivity of Tungsten Inert Gas (TIG) welding paves the way for the invention of a number of enhanced variants of it [1], such as Flux Bounded TIG (FB-TIG) welding, Activated TIG (A-TIG) welding, etc. A thin layer of activating flux is applied in A-TIG welding that helps in remarkable increase in penetration. After the inception in 1965 by Gurevich et al. [2], it had a slow progress until the beginning of 21st century when extensive research on it started. Activated flux used in A-TIG welding is a mixture of flux powders suspended in a carrier solvent. Different proponents [3-6] tried different fluxes such as titania, chromia, magnesium carbonate, magnesium oxide, manganese dioxide, calcium oxide, alumina, zirconia, etc. or a homogeneous mixture of some fluxes in different proportions. The composition of flux powder is crucial as it determines the effectiveness of the operation. Arc constriction and reversed Marangoni flow are accepted two mechanisms that simultaneously help achieve deep penetration in A-TIG welding [4, 7]. Advantages claimed by proponents of A-TIG welding process include [3-9] : (1) increased depth-of-penetration (sometimes three-fold increase in penetration compared to that of conventional TIG welding is recorded), (2) reduced distortion due to narrow arc as well as lesser heat input for constant depth-of-penetration, (3) narrow Heat Affected Zone

(HAZ) due to constricted arc, (4) reduction of problems of inconsistent weld penetration due to cast-to-cast material variations.

Slew of investigations were carried out with different flux compositions on a number of materials, but seldom research work was conducted to find the effects of heat input on the performance of A-TIG welding. The objective of the present work is to analyze variations of weld morphology and the characteristics with heat input in AC A-TIG welding (both bead-on-plate and butt joining) of 6mm thick stainless steel (grade 316L) plates using TiO_2, Cr_2O_3 and Fe_2O_3 as activating fluxes, industrially pure argon as shielding gas and a stainless steel filler. These results are also compared with that obtained for conventional TIG welding.

2.0 EXPERIMENTAL DETAILS

2.1. Base plate and filler material

In this work, stainless steel plates of size 100×40×6mm are joined by both conventional TIG and A-TIG welding using stainless steel filler rod. For joining, two plates are placed side by side (butt joint) without any edge preparation (i.e., square edge) maintaining 2mm root gap, as depicted in **Fig. 1(a)**. The composition of the base plates and also the metallurgical composition of filler material are provided in **Table 1** and **Table 2**, respectively. Before welding, the base plates are first cleaned by ethanol and are placed under welding torch backing by scrap plates (15–20mm long) to facilitate arc length adjustment and also for approach and overrun in order to obtain satisfactory welding at both ends of the joint.

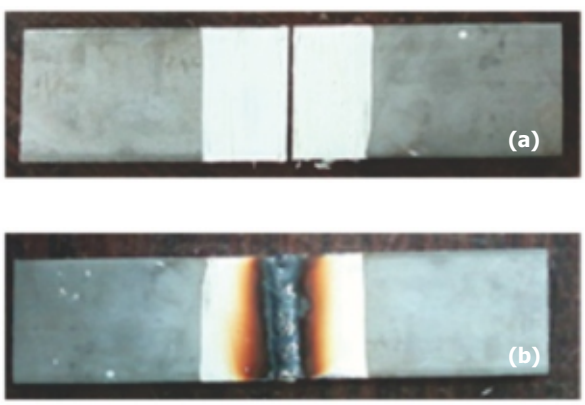

Fig. 1 : Base plates (a) before, and (b) after A-TIG welding with TiO_2 coating.

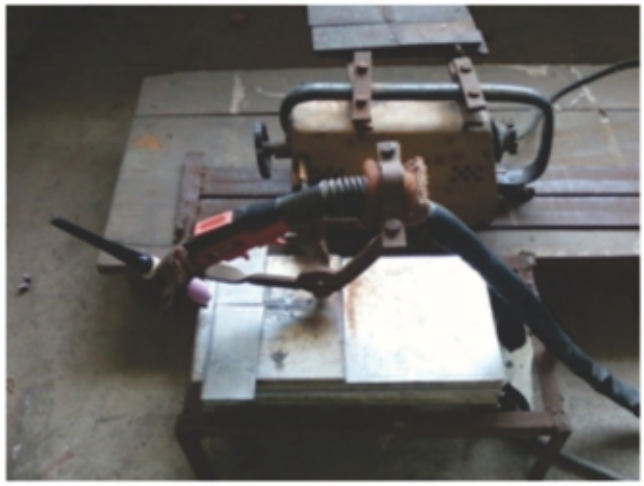

Fig.2 : Experimental set-up for butt joining of plates

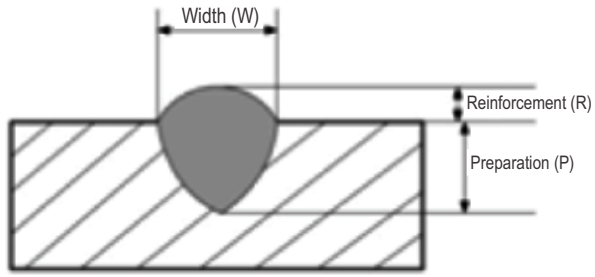

Fig.3 : Typical illustration of weld bead geometry

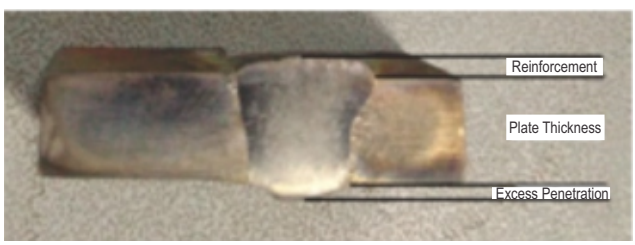

Fig. 4 : Typical representation of excessively penetrated weld joint

2.2. Flux formulation and application

Before placing the plates under the welding torch, required activated flux, mixed with acetone to form a semi-solid paste, is applied manually on cleaned and dried plates using painting brush for A-TIG welding. Thickness of this flux layer is kept constant for all the cases and is such that it just covers the plate to restrict visual appearance of plates, as portrayed in **Fig. 1**. However, measured thickness of this layer varies from a minimum of 42μm to a maximum of 58μm with an average of 53μm. Here, only three activating fluxes are employed individually (single component flux) for the sake of investigation. The fluxes are oxide of various metals, viz. titania (TiO_2), iron oxide (Fe_2O_3), and chromia (Cr_2O_3). Flux powders

Table 1 : Composition of base plate

C	Si	Mn	P	S	Cr	Mo	Ni	Co	Cu
0.014	0.418	1.293	0.028	0.014	17.153	2.054	10.203	0.381	0.240
Nb	Ti	V	W	Pb	Sn	As	Ce	B	Fe
0.074	0.019	0.066	0.037	0.003	0.002	0.004	0.012	0.008	<67.97

Table 2 : Composition of filler material

C	Si	Mn	P	S	Cr	Mo	Ni	Co	Cu
0.011	0.249	0.912	0.030	0.014	16.478	2.057	10.099	0.211	0.444
Nb	Ti	V	W	Pb	Sn	As	Ce	B	Fe
0.039	0.011	0.051	.058	0.003	0.002	0.004	0.008	0.003	<69.32

are mixed with acetone and applied on and around the faying surfaces. However, in case of conventional TIG welding, no such flux is applied.

2.3. Selection of welding parameters

From the literature review, it has been cognized that for conventional TIG welding of stainless steel (grade 316L) of 6mm thick plates, around 1.3–2.5kJ/mm heat input is required to obtain satisfactory welding. Based on this data, here current is varied from 90A to 130A with an interval of 10A, maintaining welding torch speed constant. Current chosen is AC. Both bead-on-plate and butt joining of plates are carried out using an automated vehicle. Through manual intervention, filler material was fed. The fixed as well as varying parameters used in this investigation are enlisted below.

- Following parameters/conditions have been kept constant.

Workpiece thickness	6mm
Electrode material	2% Thoriated tungsten with 2.4mm diameter
Filler material	316 Stainless Steel with 2mm diameter
Shielding gas	Commercially pure argon, Gas flow rate (15 l/min)
Welding position	Down hand with an angle of 60° with horizontal
Arc length	approximately 3mm
Welding speed	60mm/min

- Following welding parameters/conditions have been varied to investigate their influences.

Welding current	90A to 130A with an interval of 10A
Welding voltage independently	Closed circuit voltage, thus varies
Activated flux	None, TiO_2, Fe_2O_3, and Cr_2O_3

2.4. Testing of welded samples

After successful welding, the welded plates are halved by cutting cross-wise to expose the weld zone, and subsequently the exposed surface is finished by polishing successively with belt grinder, disc grinder with emery papers of grades 180, 400, 800, and 1200, and finally with cloth polisher with alumina abrasive. After obtaining the super-finished surface, the plates are etched by immersing it within Kalling's No. 2 Reagent (a homogeneous mixture of 100ml concentrated hydrochloric acid, 100ml ethanol, and 5gm cupric chloride) for about two minutes so that the clear dichotomy becomes visible in bare eyes. These specimens are then placed under tool maker's microscope to measure depth of penetration, weld-bead width, and reinforcement **(Fig. 3)** for each specimen. In some cases, at larger heat input, the weld metal penetrates full and in some cases, at meager heat input, no penetration occurs at all. For the cases of excess penetration **(Fig. 4)**, the depth of penetration is measured beyond the reverse surface of base plate also (thus sometimes give more than 6mm penetration), and there are cases where no penetration is achieved. They are treated as useless for this research.

3.0 RESULTS AND DISCUSSION

3.1. Primary observations

Experiments are carried out with five different values of current (90, 100, 110, 120, and 130A) for conventional TIG and A-TIG welding with pure TiO_2, Fe_2O_3, and Cr_2O_3 activating fluxes for bead-on-plate as well as butt joining. Thus, a total of four sets of experiment are performed with five varying current for each set, as tabulated below **(Table 3)**. Heat input values are calculated using the formula given in equation (1), where V is the closed circuit voltage in volt, I is the welding current in Ampere and S is the welding speed in mm/s. 80% electrode efficiency (η) is assumed here.

Table 3 : Sets of experiment performed

Sl.	Experiment Set	Current Set (A)	Flux Used
1	Bead-on-plate	90, 100, 110, 120, 130	1) No flux 2) TiO_2 3) Fe_2O_3 4) Cr_2O_3
2	Butt joining		

$$\text{Heat Input (HI)} = \frac{\eta VI}{S} \quad (1)$$

Although, conventional TIG welding is usually free from spatter, but the application of activated flux gives rise to mild 'oxide spatter'. The spatters are not in the form of molten metal droplet, but in the form of red hot oxide particles. Use of oxides also gives rise to formation of slag on the molten metal pool that creates a thin fragile layer on the weld metal. However, this layer automatically, forming crocodile cracks, leaves the weld zone during cooling.

3.2. Weld-bead geometry of bead-on-plate

With the help of tool maker's microscope, the weld-bead geometries, including, depth of penetration, bead width, and reinforcement of each specimen are measured for each sample. Reinforcement Form Factor (RFF) and Penetration Shape Factor (PSF) are also calculated from these measured values using equation (2) and equation (3) [10]. Weld bead geometry observed during bead-on-plate welding in all the experimental runs of experiment set I is shown in **Table 4** through **Table 7**.

Table 4 : Bead geometry for AC conventional TIG welded plate in bead-on-plate welding

Specimen No.	Heat Input (kJ/mm)	Penetration P (mm)	Width of bead W (mm)	Reinforcement R (mm)	RFF (W/R)	PSF (W/P)
SP1	1.42	1.37	6.13	4.89	1.253	4.474
SP2	1.56	1.79	6.23	4.71	1.323	3.480
SP3	1.75	2.78	6.76	3.51	1.926	2.432
SP4	1.96	3.19	7.02	2.72	2.581	2.201
SP5	2.21	3.42	7.49	2.30	3.257	2.190

Table 5 : Bead geometry for AC A-TIG (TiO_2 flux) welded plate in bead-on-plate welding

Specimen No.	Heat Input (kJ/mm)	Penetration P (mm)	Width of bead W (mm)	Reinforcement R (mm)	RFF (W/R)	PSF (W/P)
SP1	1.40	1.92	5.31	4.71	1.127	2.765
SP2	1.58	2.44	5.29	3.38	1.565	2.168
SP3	1.78	4.73	6.17	1.09	5.660	1.304
SP4	1.88	5.33	6.21	0.53	11.717	1.165
SP5	2.24	6.00	7.83	0.00	--	1.305

Table 6 : Bead geometry for AC A-TIG (Fe_2O_3 flux) welded plate in bead-on-plate welding

Specimen No.	Heat Input (kJ/mm)	Penetration P (mm)	Width of bead W (mm)	Reinforcement R (mm)	RFF (W/R)	PSF (W/P)
SP1	1.43	2.58	5.67	3.19	1.777	2.198
SP2	1.61	2.82	5.88	2.51	2.343	2.085
SP3	1.83	4.76	5.81	1.97	2.949	1.221
SP4	1.98	5.07	6.04	1.13	5.345	1.191
SP5	2.29	5.88	7.89	0.82	9.622	1.342

Table 7 : Bead geometry for AC A-TIG (Cr_2O_3 flux) welded plate in bead-on-plate welding

Specimen No.	Heat Input (kJ/mm)	Penetration P (mm)	Width of bead W (mm)	Reinforcement R (mm)	RFF (W/R)	PSF (W/P)
SP1	1.50	1.45	6.43	5.11	1.258	4.434
SP2	1.73	1.94	7.02	4.51	1.557	3.618
SP3	1.93	2.33	7.13	4.02	1.774	3.060
SP4	2.18	2.76	7.42	3.78	1.963	2.688
SP5	2.47	3.18	7.92	3.71	2.135	2.490

$$\text{Reinforcement Form Factor (RFF)} = \frac{\text{Width of Weld Head (W)}}{\text{Reinforcement (R)}} \quad (2)$$

$$\text{Penetration Shape Factor (PSF)} = \frac{\text{Width of Weld Head (W)}}{\text{Depth of Penetration (P)}} \quad (3)$$

3.3. Weld-bead geometry of butt joined plates

Weld-bead geometry is also observed on butt joined plates, and results are given in **Table 8** through **Table 11**.

Table 8 : Bead geometry for AC conventional TIG welded plate in butt joining

Specimen No.	Heat Input (kJ/mm)	Penetration P (mm)	Width of bead W (mm)	Reinforcement R (mm)	RFF (W/R)	PSF (W/P)
SP1	1.34	–	–	–	–	--
SP2	1.59	2.13	5.61	4.32	1.299	2.634
SP3	1.80	2.56	6.33	4.07	1.555	2.473
SP4	2.03	2.91	6.74	3.67	1.836	2.316
SP5	2.17	3.06	6.90	3.21	2.149	2.255

Table 9 : Bead geometry for AC A-TIG (TiO_2 flux) welded plate in butt joining

Specimen No.	Heat Input (kJ/mm)	Penetration P (mm)	Width of bead W (mm)	Reinforcement R (mm)	RFF (W/R)	PSF (W/P)
SP1	1.43	–	–	–	–	--
SP2	1.70	3.29	6.08	2.61	2.329	1.848
SP3	1.83	5.13	6.26	2.01	3.114	1.220
SP4	2.07	5.89	6.58	0.86	7.651	1.117
SP5	2.33	6.32	6.79	0.00	–	1.074

Table 10 : Bead geometry for AC A-TIG (Fe_2O_3 flux) welded plate in butt joining

Specimen No.	Heat Input (kJ/mm)	Penetration P (mm)	Width of bead W (mm)	Reinforcement R (mm)	RFF (W/R)	PSF (W/P)
SP1	1.41	–	–	–	–	--
SP2	1.67	2.31	6.23	3.11	2.003	2.696
SP3	1.89	4.28	6.56	1.84	3.565	1.533
SP4	2.10	5.17	6.82	1.07	6.373	1.319
SP5	2.27	5.82	7.04	0.75	9.387	1.209

Table 11 : Weld bead geometry for AC A-TIG (Cr_2O_3 flux) welded plate (butt joining)

Specimen No.	Heat Input (kJ/mm)	Penetration P (mm)	Width of bead W (mm)	Reinforcement R (mm)	RFF (W/R)	PSF (W/P)
SP1	1.46	–	–	–	–	--
SP2	1.68	–	–	–	–	--
SP3	1.91	2.38	6.22	4.33	1.436	2.613
SP4	2.14	2.79	6.81	3.94	1.728	2.440
SP5	2.38	3.15	7.59	3.52	2.156	2.409

3.4 Variation of weld bead geometry with heat input

It is axiomatic from the **Fig. 5** that with increase in heat input, penetration tends to increase except at few experimental runs. This is due to the fact that higher heat input causes sufficient melting of both the base plate and filler metal, thereby improving fluidity and wettability that guides the molten metal to penetrate deeper as well as to spread wider. It is also evident that at lower level of heat input, penetration achieved for conventional TIG and A-TIG welding is almost the same; however, at higher heat input, TiO_2 and Fe_2O_3 flux based A-TIG welding shows remarkable enhance in achievable penetration because of the arc constriction phenomenon caused by reverse Marangoni effect. TiO_2 flux gives 6.00mm and 6.32mm penetration with heat input of 2.24kJ/mm in bead-on-plate welding and 2.33kJ/mm in butt joining, respectively; whereas conventional TIG welding gives a maximum of 3.42mm penetration in this range of heat input. On the other hand, Cr_2O_3 flux is found to be ineffective in this purpose; even it gives inferior result as compared to conventional TIG welding. As expected, width of the weld bead is also found to increase with the heat input **(Fig. 6)** both in conventional TIG and A-TIG welding.

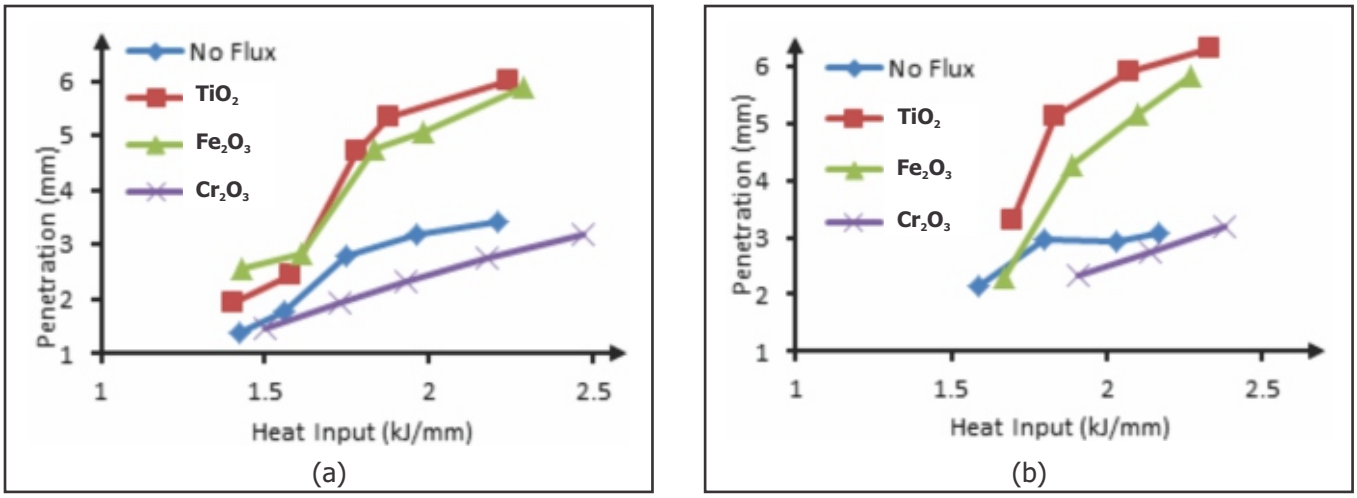

Fig.5 : Plots of variation of penetration with heat input in (a) bead-on-plate and (b) joining

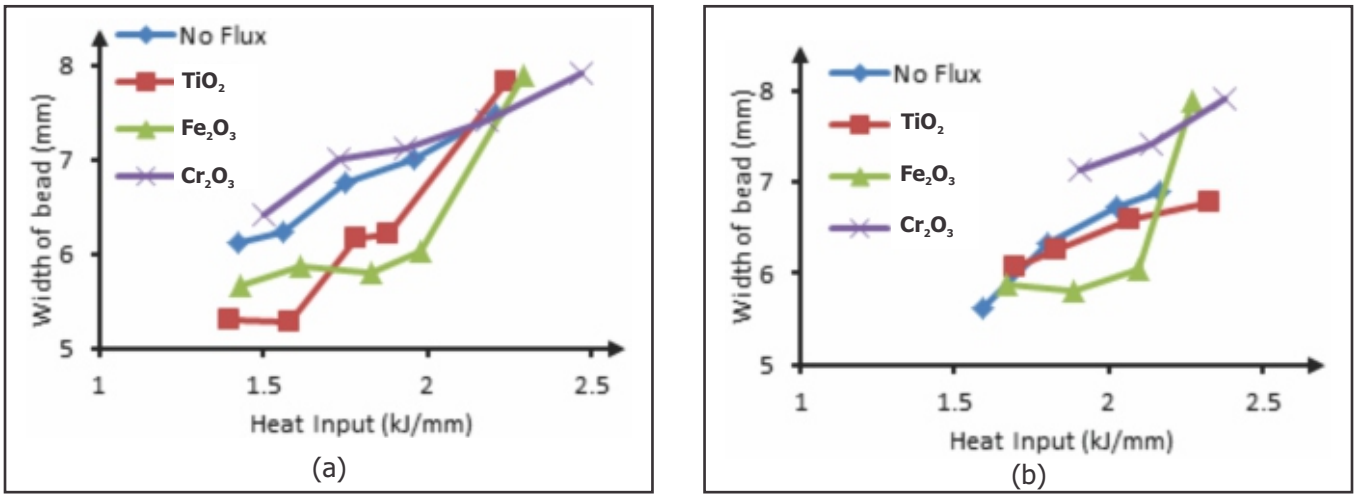

Fig.6 : Plots of variation of bead width with heat input in (a) bead-on-plate and (b) joining

Since filler metal deposition rate is unchanged, so increase in penetration as well as bead width should result in reduced reinforcement-this fact can be easily noticed from the reinforcement variation, as depicted in **Fig. 7**. Since TiO_2 and Fe_2O_3 flux based A-TIG welding exhibits deeper penetration, and at the same time, wider weld bead at higher ranges of heat input, it displays reinforcement quite small and sometimes zero. It also implies that further increase in heat input for welding 6mm plates can lead to defective welding if filler metal deposition rate is not increased. Cr_2O_3 flux based A-TIG welding, however, shows negligible reduction in reinforcement. It is also observed that for butt joining of plates, a little higher heat input is required in order to achieve proper melting of base plates. Thus, no joining takes place at lower range of heat input, as revealed from **Fig. 7(b)**.

Reinforcement Form Factor (RFF) and Penetration Shape Factor (PSF) indicate the relative change of one weld bead parameter with respect to another. Increasing trend of RFF implies that rate of decrease in reinforcement with increase in heat input is much higher than the rate of increase of weld bead width. On the other hand, decreasing trend of PSF implies that rate of increase of penetration with increase in heat input is much higher than the rate of increase of weld bead width.

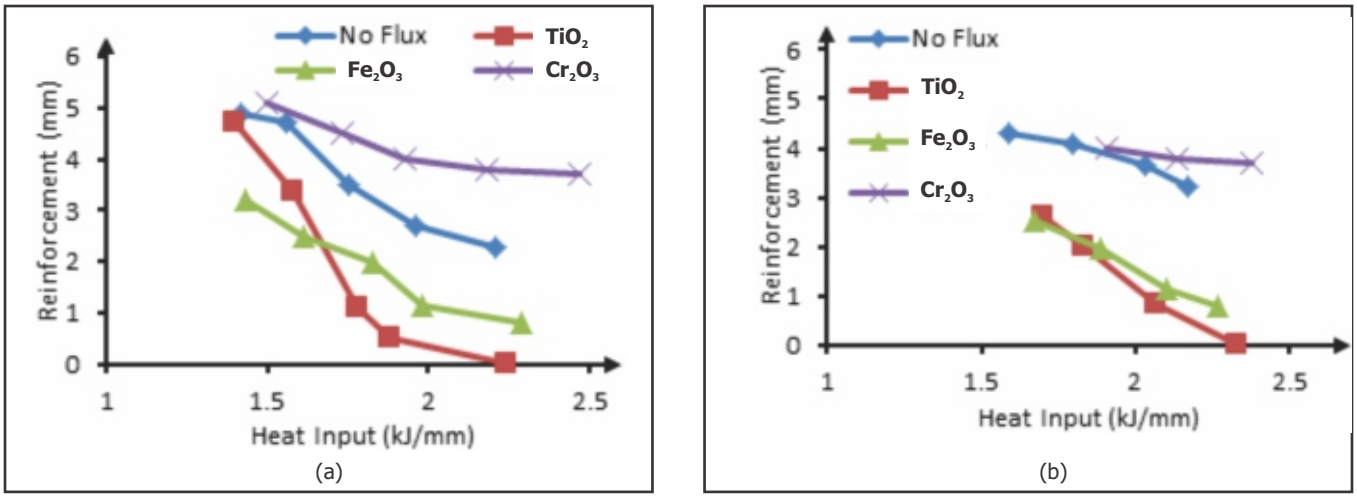

Fig.7 : Plots of variation of reinforcement with heat input in (a) bead-on-plate and (b) joining

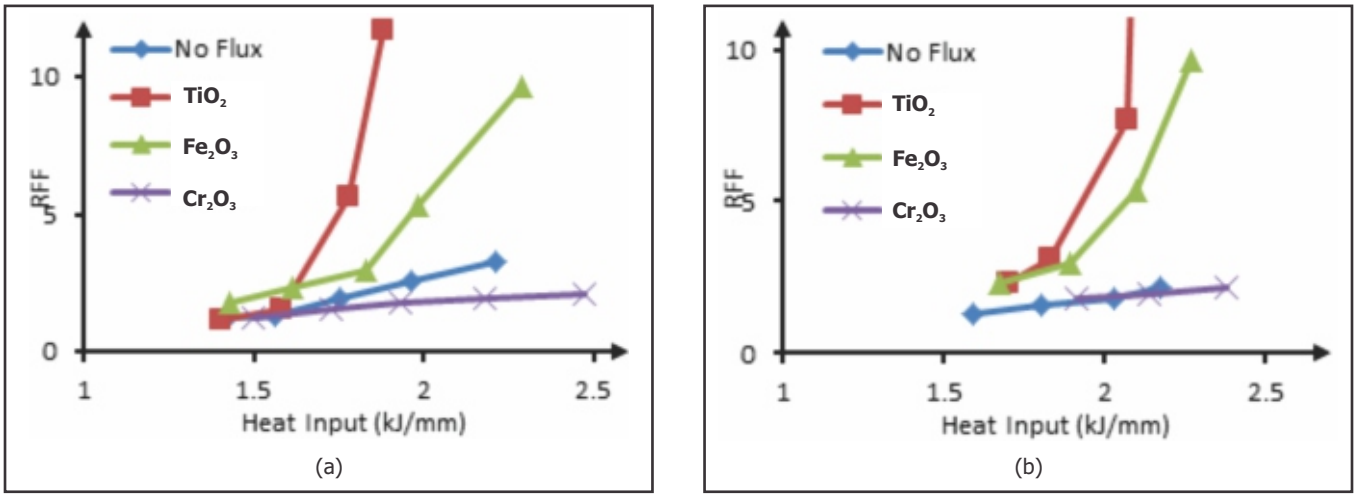

Fig.8 : Plots of variation of RFF with heat input in (a) bead-on-plate and (b) joining

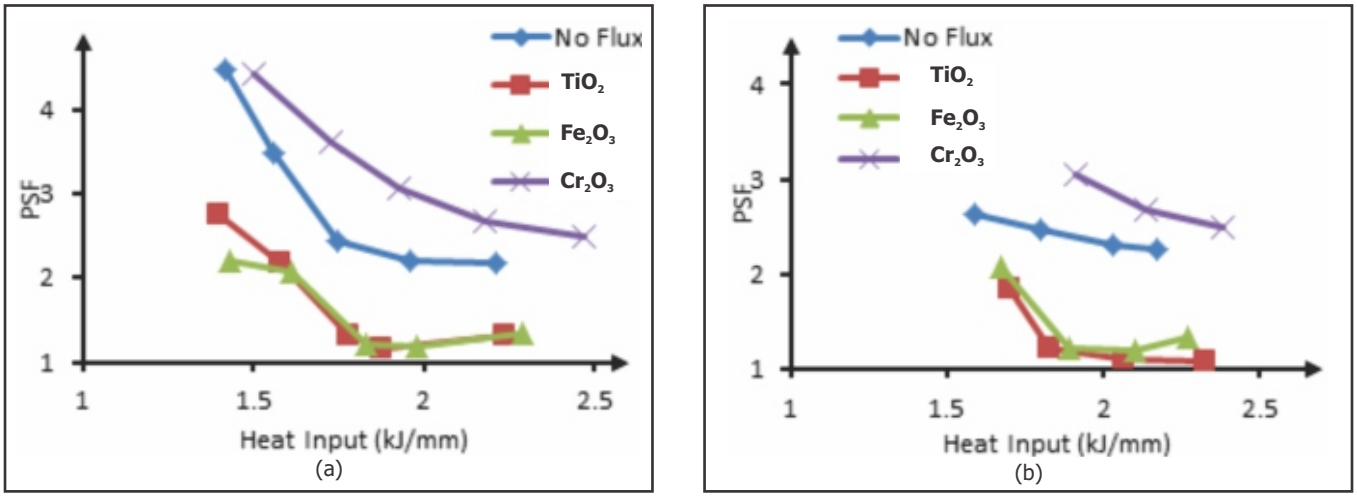

Fig.9 : Plots of variation of PSF with heat input in (a) bead-on-plate and (b) joining

In A-TIG welding with TiO_2 and Fe_2O_3 flux at higher ranges of heat input, the RFF is found to be high whereas PSF is found to be low (sometime zero). These are the results of steep decrease of reinforcement or steep increase in penetration.

4.0 CONCLUSION

On the basis of the results obtained in this experimental investigation, following conclusions can be drawn:

- For both TIG and A-TIG welding (with TiO_2, Fe_2O_3 and Cr_2O_3 fluxes) with AC polarity, proper fusion of 6mm 316L stainless steel base plate can be achieved only at the heat input values higher than about 1.4kJ/mm; except for Cr_2O_3 flux, for which higher level of heat input i.e., about 1.9kJ/mm is necessity to attain satisfactory fusion of base plate. Butt joining of plates requires slightly high heat input.
- Utilization of TiO_2 flux results in deeper penetration, which, in some cases with higher heat input, reaches more than twice the penetration obtained by conventional TIG welding, and in other cases also, it gives appreciable increase in penetration. TiO_2 flux is also effective in reducing weld bead width as it helps in constricting arc.
- Fe_2O_3 flux also shows remarkable increase in penetration that may reach up to 90% increase with higher heat input. This is also effective in reducing weld bead width.
- Cr_2O_3 flux is recorded effective neither in enhancing penetration nor in reducing weld bead width; rather, it decreases the penetration achievable by conventional TIG welding by an appreciable amount.

ACKNOWLEDGEMENT

The present paper is a revised version of an article presented in the International Congress (IC-2017) of the International Institute of Welding held in Chennai on December 07-09 2017 and organized by the Indian Institute of Welding.

REFERENCE

[1] Lin HS and Wu TM (2012); Effects of activating flux on weld bead geometry of inconel 718 alloy TIG welds, Mat and Manuf Proc, 27, pp.1457-1461.

[2] Gurevich SM, Zamkov VN and Kushnirenko NA (1965); Improving the penetration of titanium alloys when they are welded by argon tungsten arc process, Avtomatich Svarka, 9(4).

[3] Howse DS and Lucas W (2000); Investigation into arc constriction by active fluxes for tungsten inert gas welding; Sc and Tech of Welding and Joining, 5(3), pp.189-193.

[4] Tseng KH (2013); Development and application of oxide-based flux powder for tungsten inert gas welding of austenitic stainless steels, Powder Tech, 233, pp.72-79;.

[5] Kuo CH, Tseng KH and Chou CP (2011); Effect of activated TIG flux on performance of dissimilar welds between mild steel and stainless steel, Key Engg Mat, 479, pp.74-80.

[6] Dey HC, Albert SK, Bhaduri AK and Mudali UK (2013); Activated flux TIG welding of titanium, Welding in the World, 57(6), pp.903-912.

[7] Magudeeswaran G, Nair SR, Sundar L and Harikannan N (2014); Optimization of process parameters of the activated tungsten inert gas welding for aspect ratio of UNS S32205 duplex stainless steel welds, Defence Tech, 10(3), pp.251-260.

[8] Sambherao AB (2013); Use of activated flux for increasing penetration in austenitic stainless steel while performing GTAW, Int J Emerging Tech and Adv Engg, 3(12).

[9] Roy S, Samaddar S, Nasim Uddin Md., Hoque A, Mishra S and Das S (2017); Effect of activating flux on penetration in ATIG welding of 316 stainless steel, Indian Welding Journal, 50(4), pp. 72-80.

[10] Mondal A, Saha MK, Hazra R and Das S (2016); Influence of heat input on weld bead geometry using duplex stainless steel wire electrode on low alloy steel specimens, Cogent Engg, 3(1), pp.1143598/1-14.